Failure Analysis and Countermeasures of SCM435 High-Tension Bolt of Three-Step Injection Mold

Seo-Hyun Yun[1], Ki-Woo Nam[2*]

〈Abstract〉

When injection mold is repeatedly used for mass production, fatigue phenomenon due to cyclic stress may occur. The surface and interior of structure might be damaged due to cyclic stress or strain. The objective of this study was to analyze failure of SCM435 high-tension bolts connecting upper and lower parts of a three-stage injection molding machine. These bolts have to undergo an accurate heat treatment to prevent the formation of chromium carbide and the action of dynamic stresses. Bolts were fractured by cyclic bending stress in the observation of ratchet marks and beach marks. Damaged specimen showed an acicular microstructure. Impurity was observed. Chromium carbide was observed near the crack origin. Both shape parameters of the Vickers hardness were similar. However, the scale parameter of the damaged specimen was about 20% smaller than that of the as-received specimen. Much degradation occurred in the damaged specimen. Bolts should undergo an accurate heat treatment to prevent the formation of chromium carbide. They must prevent the action of dynamic stresses. Bolts need accurate tightening and accuracy of heat treatment and screws need compression residual stress due to peening.

Keywords : Failure Analysis, Fatigue Limit, Injection Mold, SCM435 High-Tension Bolt

1 Dept. of Marine Convergence Design Engineering, Pukyong National University
2* Dept. of Materials Science and Engineering, Pukyong National University
E-mail: namkw@pknu.ac.kr

1. Introduction

Injection moulding is a manufacturing process for producing parts by injecting molten material with malleability and fluidity into a mould [1]. Injection molding is essential for mass production of products. Since the mold is repeatedly used for mass production, damage may occur due to cyclic stress [2]. In general, fatigue can damage the surface or the inside of a member due to cyclic stress or strain. Damage is a problem between atoms. Defects and dislocations of crystal lattice are important variables for fatigue. In other words, if low stress acts repeatedly, materials can be damaged. Failure analysis has been conducted by many researchers because of the safety and longevity of a structure [3-9].

The objective of this study was to perform damage analysis of SCM435 high-tension bolts connecting upper and lower parts of a three-stage injection molding machine. Countermeasures are also suggested. Fracture surface and components of damaged material were examined by Scanning Electron Microscope (SEM) and Energy Dispersive X-Ray Spectroscopy (EDS). Microstructure and hardness of as-received material and damaged material were measured and compared.

2. Damaged material and analysis method

Damage material used in this study was SCM435 high-strength bolt connecting upper and lower molds of a three-stage injection mold. The bolt of the three-stage injection mold fixes the left and right tension links. The tension link is a device for controlling the distance of the three-stage mold. It is needed to prevent separation of the mold. It exists to remove the product on the mold moving shaft. The bolt will be subjected to tension load and torsional loads. The three-stage injection mold does not have a connection between the upper mold and the lower mold. However, the tension link is installed so that the lower mold and the upper mold can be fixed for convenience in the field. Total weight of the mold was 211 kg. The lower part weight 90kg. The lower part was fixed with four bolts. SCM435 is a low alloy steel of chromium with molybdenum added. It has excellent hardenability, hot workability, weldability, and creep resistance. SCM435 is widely used for high-tension bolts and crank shafts. It is also used for pipes of high temperature and high pressure.

Causes of damage were determined by macroscopic observation. Microstructure observation was done using a metallic microscope. Fracture surface observation was performed using a Scanning Electron Microscope (SEM, S-2400, HiTachi, Japan).

Component investigation of the fracture surface was performed by Energy Dispersive X-Ray Spectroscopy (EDS, Kevex Ltd., Sigma). Hardness was measured with a Vickers hardness tester (HV-114, Mitutoyo). Structures of as-received specimens and damaged specimens were etched with Nital 3% solution after mirror polishing. Vickers hardness was measured 20 times at an indentation load of 2 kg and an indentation time of 6 seconds. Vickers hardness was analyzed for material properties using Weibull analysis. Fatigue limit of the damaged material was evaluated using equivalent crack length.

3. Results and discussion

Fig. 1 shows micro structures of as-receives specimens and damaged specimens. Fig. 1(a) shows bainite structure by heat treatment. Fig. 1(b) shows acicular microstructure. Impurity was observed.

Fig. 2 shows results of fracture surface observation by SEM. Fig. 2(a) shows the whole fracture surface. ① is origin of fracture. ② shows many beach marks as characteristic of fatigue fracture. Beach marks indicate stripes that appear on the fracture surface by oxidizing the crack tip due to variable loads. ③ indicates final breaking part. The arrow indicates crack propagation direction. (b) is enlarged crack origin. Many ratchet marks were observed on the fatigue fracture surface [10]. Ratchet marks indicate that small cracks have initiated on multiple planes. Small tear steps or shear walls often occur near the origin of multiple fatigue cracks. This disappears as the crack propagates to inside direction. Many beach marks were observed due to changes in environment and load. This indicates that the bolt is fractured by fatigue. (c) is an enlarged photograph in order to confirm the origin of a crack. The outside of the fracture surface had many crack origins. It can be seen that the crack has propagated due to fatigue between ratchet marks (dotted line in the figure). In addition, beach marks due to crack propagation could be seen between ratchet marks.

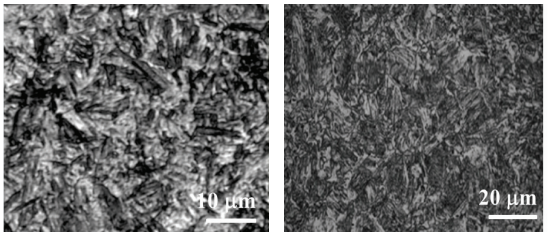

(a) (b)

Fig. 1 Metallurgical structure of damaged specimen. (a) As-received specimen, (b) Damaged specimen

Fig. 3 shows results of EDS analysis of as-received specimen and damaged specimen. As-received specimens were found to contain Si, Cr, and Mn as main components of SCM435. Cr and Mn were more detected in the damaged specimen. Table 1 shows components in weight% and atomic%. The amounts of Cr and O in the damaged specimen were higher than those in the

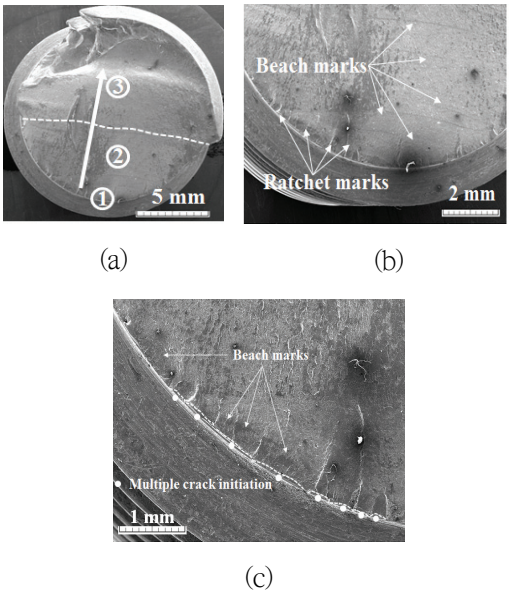

Fig. 2 Appearance of fractured surface observed by SEM

as-received specimen. Physical properties can change depending on contents of Fe and Mn. As Cr is used for a long time, Cr precipitates at grain boundaries and forms chromium carbides (mainly $Cr_{23}C_6$). When surrounding chromium elements are gathered at the grain boundary due to the formation of carbide, chromium concentration around the grain boundary is locally lowered by the amount. This is called sensitization. Chromium carbide is embrittled and easily fractured by external force [11,12]. As Cr moves around the chromium carbide, the strength becomes weak.

Fig. 4 compares Vickers hardness of as-received and damaged specimens. Hardness values of as-received specimen and damaged specimen were HV467.5~517.5 and HV370.5 ~407.5, respectively. This can be seen that

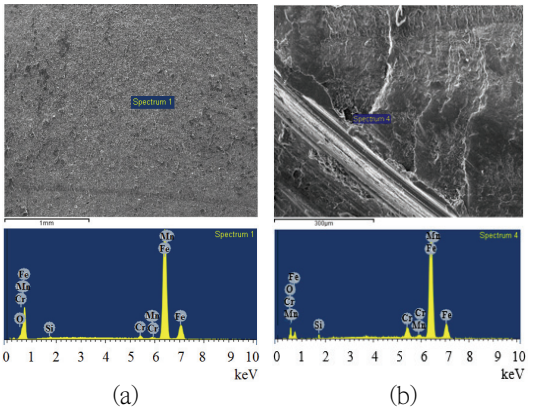

Fig. 3 Results of EDS analysis. (a) As-received specimen. (b) Damaged specimen

Table 1. Elements of as-received specimen and damaged specimen

As-received	Element	O K	Si K	Cr K	Mn K	Fe K	Totals
	wt.%	1.40	0.20	1.13	0.87	96.39	100
	at.%	4.72	0.39	1.17	0.85	92.87	
Damaged	Element	O K	Si K	Cr K	Mn K	Fe K	Totals
	wt.%	2.97	0.33	4.54	1.09	91.07	100
	at.%	9.61	0.43	4.52	1.02	84.41	

the hardness of the material does not have a constant value, but a distribution. Characteristic of the hardness distribution can be explained by Weibull distribution [13-16].

The Weibull plot (linear-regression method) is the most common one. Cumulative distribution function that gives the probability of P at the Vickers hardness HV can be expressed with the following equation (1):

$$P = 1 - \exp\left[-\left(\frac{x}{\beta}\right)^{\alpha}\right] \quad (1)$$

Where P is the probability of the Vickers hardness HV; α and β are shape parameter

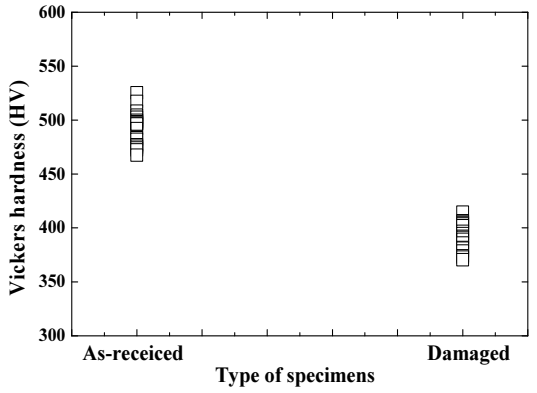

Fig. 4 Vickers hardness values of as-received specimen and damaged specimen

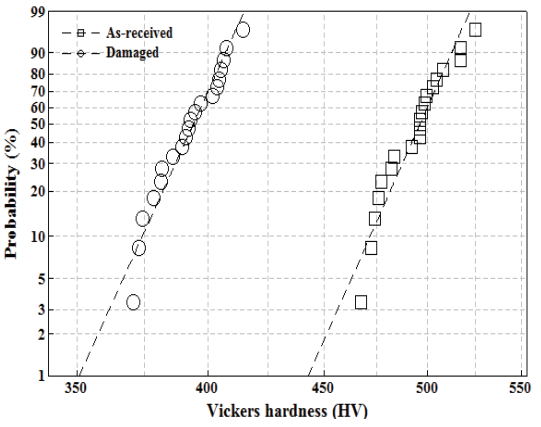

Fig. 5 Weibull plot of Vickers hardness

and scale parameter, respectively; and x is Vickers hardness HV.

The scale parameter β describes Vickers hardness HV in 63.2% of the specimen, while shape parameter α gives indication of data scattering. A higher value of α indicates a smaller variation in the examined property and a high degree of material homogeneity.

Fig. 5 shows Vickers hardness of as-received specimen and damaged specimen according to Weibull probability. Since Vickers hardness is expressed as a straight line, it is applicable to the Weibull probability distribution. Table 2 shows shape parameter and scale parameters of the Weibull distribution function as estimated from the Vickers hardness of the as-received specimen and the damaged specimen. The table also shows mean, standard deviation (Std), and coefficient of variation(COV).

Shape parameters of as-received and damaged specimens were similar to each other. For damaged specimens, the degradation was uniformly distributed throughout. However, scale parameter(398) of the damaged material with characteristic life at 63.2% was about 20% smaller than the as-received specimen(501.3). This means that the characteristic life is reduced due to degradation.

The injection mold apparatus is supported by four bolts. The two upper bolts are affected by the lower mold. The weight of lower mold is about 882N. One bolt is subjected to a load of about 441N. Bending stress is 184MPa because the length of the bolt is 5cm. The fatigue limit of SCM435 steel studied by Takaki [17] and Suh [18] et

Table 2. Weibull parameters estimated from Vickers hardness

Specimen / Parameter	Shape parameter	Scale parameter	Mean/Std /COV
As-received	37.2	501.3	494.2/16.2 /0.033
Damaged	36.4	398.0	392.3/12.9 /0.033

al. was 440MPa for non-nitride specimen, 540~580MPa for nitride specimen, and 500 MPa for heat-treated specimen. Therefore, the stress of the mold bolt used in this study was 42% of the non-nitride specimen, 34~32% of the nitride specimen, and 37% of the heat-treated specimen. Thus, the applied stress was lower than stress of the fatigue limit. However, the bolt has stress concentration on the screw. Brittle Cr carbide was formed by long time operation. Thus, unexpected dynamic load was applied on the screw. As shown in Fig. 2, a ratchet mark occurred in the outside of the bolt. Therefore, bolts require heat treatment in which Cr carbide is not easily formed, and the reduction of dynamic stresses.

As mentioned above, let's think a possibility that the one bolt breaks at a stress of 184MPa. The stress intensity factor K in the case where an infinite plate has a penetration crack of arbitrary length (2c) can be evaluated with Eq. (2):

$$K = \sigma_B \sqrt{\pi c} \tag{2}$$

On the other hand, the stress intensity factor K of semi-elliptical surface cracks in the finite plate can be evaluated by the Newman-Raju equation [19]. As shown in Fig. 6, when bending stress is applied to the semi-elliptical surface crack of length (2c) and depth (a) on the finite plate, the stress intensity factor K is given by Eq. (3):[20]

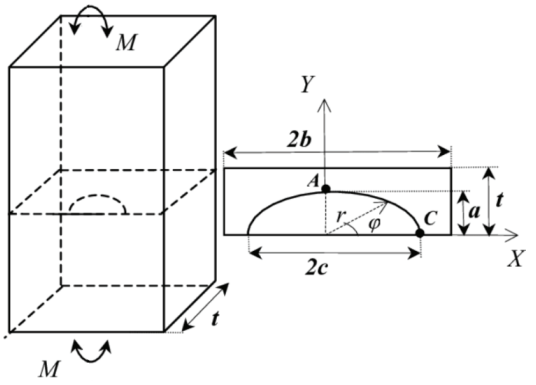

Fig. 6 Schematic illustration of a finite plate containing a semi-circular crack

$$K = \frac{H\left(\frac{a}{t},\frac{a}{c},\frac{c}{b},\phi\right)F\left(\frac{a}{t},\frac{a}{c},\frac{c}{b},\phi\right)}{\sqrt{Q\left(\frac{a}{c}\right)}}\sigma_B\sqrt{\pi a} = \beta\sigma_B\sqrt{\pi a} \tag{3}$$

Where F and Q are shape correction factors, t is the thickness of the finite plate, b is a half of the finite plate width, and ϕ is the angle of the tip of the semi-elliptical surface crack. β represents shape correction factors collectively.

When the through-crack length of the infinite plate showing the same K at the same stress is expressed as the equivalent crack length, Eqs. (2) and (3) are satisfied by Eq. (4).

$$K = \sigma_B\sqrt{\pi c_e} = \beta\sigma_B\sqrt{\pi a} \tag{4}$$

From Eq. (4), the relationship between and a is given by Eq. (5):

$$\sqrt{c_e} = \beta\sqrt{a} \tag{5}$$

Therefore, crack-size dependence of the threshold stress intensity factor on semi-elliptical surface cracks of the finite plate can be evaluated by Eq. (6) by substituting into Eq. (5) instead of c in Eq. (2):

$$\Delta K_{th}^{R} = 2\beta\Delta\sigma_{w}^{R}\sqrt{\frac{a}{\pi}}\cos^{-1}\left\{\frac{\pi}{8\beta^{2}a}\left(\frac{\Delta K_{th(l)}^{R}}{\Delta\sigma_{w}^{R}}\right)^{2}+1\right\}^{-1} \quad (6)$$

Where β is function of φ. K varies depending on the angle of the crack tip that evaluates K. is fatigue limit of smooth specimen. is threshold stress intensity factor which has a very long penetration crack in the infinite plate. Since the right side of Eq. (7) is a constant, the relation between and can be obtained from the second term [20].

$$c_{0}\left\{\sec\left(\frac{\pi\Delta\sigma_{wc}^{R}}{2\Delta\sigma_{w}^{R}}\right)-1\right\}=\frac{\pi}{8}\left(\frac{\Delta K_{th(l)}^{R}}{\Delta\sigma_{w}^{R}}\right)^{2} \quad (7)$$

Heat treatment conditions of SCM435 steel are as follows: quenching (1.8 ks at 855℃ + oil cooling) and annealing (3.6 ks at 600℃ + water cooling) [18]. The fatigue limit of the specimen obtained by heat treatment was 500MPa [17,18]. The threshold stress intensity factor of the long crack obtained at yield stress of 902MPa for the as-received specimen of SCM435 was 5.6MPa [21]. Fig. 7 shows fatigue limits obtained by substituting these values into Eq. (7). Fig. 7(a) shows fatigue limit of the surface cracks for depth cracks. Fig. 7(b) shows fatigue limit for depth cracks. Fatigue limits are shown for aspect ratios of 1.0, 0.6, 0.3, and 0.1. In the figure, applied stress 184MPa on the bolt is shown as dotted line. It could be seen that the fatigue limit decreased rapidly as crack size increased. This tendency was different depending on surface cracks and depth cracks. Surface cracks decreased in the order of crack aspect ratios of 1.0, 0.6, 0.3, and 0.1, while crack depths decreased in the order of 0.1, 0.3, 0.6, and 1.0. Table 3 shows the crack aspect ratio of the crack size at the point where the applied stress 184MPa (dotted line) of the bolt and fatigue limit meets.

In Table 3, fractures of SCM435 bolts occurred at small size of surface and depth cracks. The crack size at which fracture occurs are shown in bold. Here, the surface crack of As = 0.1 showed crack size of 1 mm or more. Fractures occurred at surfaces of As = 1.0 and depth of As = 0.6, 0.3, and 0.1. Therefore, in this study, it was judged that fractured bolts occurred larger than the size of surface and depth cracks shown in the table due to cyclic load or large load. In order to control such fracture, accurate tightening of bolts, accuracy of heat treatment, and screws are required for compression residual stress due to peening.

Table 3. Crack size of fatigue limit for applied stress of 323MPa at each aspect ratio

Crack \ As	1.0	0.6	0.3	0.1
Surface	**0.499**	0.511	0.716	〈 1
Depth	0.702	**0.394**	**0.268**	**0.219**

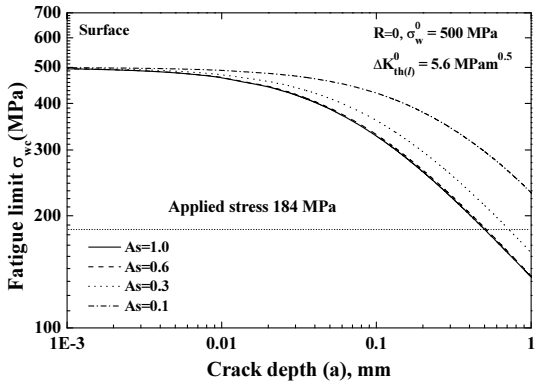

(a)

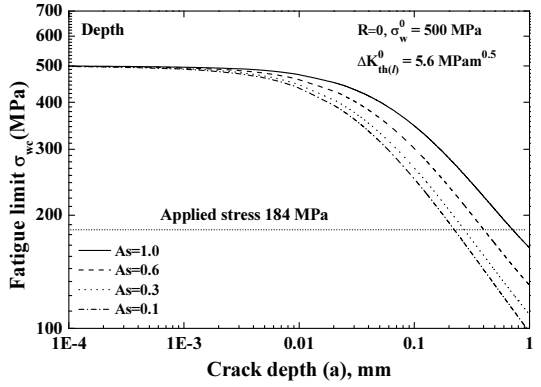

(b)

Fig. 7 Relationship of fatigue limit and crack size. (a) Surface crack, (b) Depth crack

4. Conclusions

This study conducted failure analysis of damaged SCM435 bolts connecting upper and lower parts of the three-stage injection mold. Results are as follows.

(1) Bolts were fractured by cyclic bending stress in the observation of ratchet marks and beach marks.

(2) Damaged specimen showed an acicular microstructure. Impurity was observed. Chromium carbide was observed near the crack origin.

(3) Both shape parameters of the Vickers hardness were similar. However, the scale parameter of the damaged specimen was about 20% smaller than that of the as-received specimen. Much degradation occurred in the damaged specimen.

(4) Bolts should undergo an accurate heat treatment to prevent the formation of chromium carbide. They must prevent the action of dynamic stresses.

(5) Bolts need accurate tightening and accuracy of heat treatment. Screws require compression residual stress due to peening.

References

[1] J. S. Kim and T. W. Park, 2015, “NCS-Based Injection Mold”, Bogdoo. co. Ltd.

[2] L. O. A. Affonso, 2006, “Fatigue Fractures”, Machinery Failure Analysis Handbook, pp. 43-53.

[3] Q. Hu, K. Song and X. Jiang, 2012, “Research of Fatigue Stress Cracking for Injection Mold Cavity Based on Ansys Workbench”, Applied Mechanics and Materials, Vols. 217-219, pp. 1757-1761.

[4] J. K. Kim and C. S. Lee, 2013, “Fatigue life estimation of injection mold core using simulation-based approach”, International Journal of Automotive Technology, Vol. 14, Issue 5, pp. 723-729.

[5] K. W. Nam, C. S. Kim and S. H. Ahn, 2016, “Damage Analysis of Degraded Slitting Knife”,

International Journal of Engineering Sciences & Research Technology, Vol. 5, No. 9, pp. 153-159.

[6] K. W. Nam, C. S. Kim and S. H. Ahn, 2016, "A study on wear damage of SKD11 steel material for a cutting mold jig" Journal of the Korean Society for Power System Engineering, Vol. 20, No. 5, pp. 5-13.

[7] L. Lu, J. Zhou, R. Iyer, J. Webb, D. Woods and T. Pietila, 2017, "Fatigue Life Prediction of Injection Molding Tool", SAE Technical Paper 2017-01-0340.

[8] A. T. Miller, D. L. Safranski, K. E. Smith, D. G. Sycks, R. E. Guldberg and K. Gal, 2017, "Fatigue of injection molded and 3D printed polycarbonate urethane in solution", Polymer, Vol. 108, pp. 121-134.

[9] C. S. Kim, K. W. Nam and S. H. Ahn, 2017, "Failure Analysis and Weibull Statistical Analysis according to Impact Test of the Angular Pin for Injection Molding Machines", Journal of the Korean Society for Power System Engineering, Vol. 21, No. 3, pp. 37-44.

[10] Sh. Zangeneh, M. Ketabchi and A. Kalaki, 2014, "Fracture failure analysis of AISI 304L stainless steel shaft", Engineering Failure Analysis, Vol. 36, pp. 155-165.

[11] J. W. Kim, S. H. Kim, J. H. Jeong, Y. S. Kim and K. W. Nam, 2014, "Cause and solution of damage on STS310S tube for heat exchange devices", Transactions of the KSME (A), Vol. 39, No. 2, pp. 187-193.

[12] P. Atanda, A. Fatudimu and O. Oluwole, 2010, "Sensitisation Study of Normalized 316L Stainless Steel", Journal of Minerals & Materials Characterization & Engineering, Vol. 9, No.1, pp. 13-23.

[13] W. Weibull, 1951, "A statistical distribution function of wide applicability", J. Appl. Mech. Trans. ASME, Vol. 18, No. 3, pp. 293-297.

[14] S. H. Ahn, S. C. Jeong and K. W. Nam, 2016, "Weibull Statistical Analysis on Mechanical Properties of Immersed Silicon Carbide in Acidic and Alkaline Solution", Journal of Ceramic Processing Research. Vol. 17, No. 9, pp. 994-998.

[15] S. H. Ahn, C. Y. Kang and K. W. Nam, 2017, "Weibull Distribution for Vickers Hardness of Peened ZrO2 Ceramics According to Shot Sizes", Journal of Ceramic Processing Research. Vol. 18, No. 6, pp. 425-430.

[16] I. D. Park, K. W. Nam and C. Y. Kang, 2018, "Shear Strength of Ball Studs According to the Resistance Welding Conditions & Reliability Testing Based on the Weibull Distribution Function", Journal of Mechanical Science and Technology, Vol. 32, No. 12, pp. 5647-5652.

[17] S. Takagi, N. Nakamura, A. Sano and Y. Tonozuka, 2013, "UKA "Fatigue Strength Property of Nitrided JIS-SCM435 Steel", Research Report of Kanagawa Institute of Industrial Science and Technology, No.19, pp. 6-9.

[18] M. S. Suh, C. M. Suh and Y. S. Pyun, 2013, "Very high cycle fatigue characteristics of a chrome-molybdenum steel treated by ultrasonic nanocrystal surface modification technique", Fatigue & Fracture of Engineering Materials & Structures, Vol. 36, No. 8, pp. 769-778.

[19] J. C. Newman Jr, and I. S. Raju, 1981, "An empirical stress-intensity factor equation for the surface crack", Engineering Fracture Mechanics, Vol. 15, No. 1-2, pp. 185-192.

[20] K. Ando, R. Fueki, K. W. Nam, K. Matsui and K. Takahashi, 2019, "A Study on the Unification of the Threshold Stress Intensity Factor for Micro Crack Growth", Japan Society of Spring Engineers, Vol. 64, pp. 39-44.

[21] Y. Kitsunai, 1980, "Effect of microstructure on fatigue crack growth behavior of carbon steels", The Society of Materials Science of Japan, Vol. 29, pp. 1018-1023.

(Manuscript received May 27, 2020;
revised June 19, 2020; accepted June 29, 2020)